Minimizing tip-sample forces and enhancing sensitivity in atomic force microscopy with dynamically compliant cantilevers

Aliasghar Keyvani, Hamed Sadeghian, Mehmet Selman Tamer, Johannes Frans Loodewijk Goosen, and Fred van Keulen

Citation: Journal of Applied Physics **121**, 244505 (2017); doi: 10.1063/1.4990276
View online: http://dx.doi.org/10.1063/1.4990276
View Table of Contents: http://aip.scitation.org/toc/jap/121/24
Published by the American Institute of Physics

Minimizing tip-sample forces and enhancing sensitivity in atomic force microscopy with dynamically compliant cantilevers

Aliasghar Keyvani,[1,2] Hamed Sadeghian,[2,a)] Mehmet Selman Tamer,[1,2]
Johannes Frans Loodewijk Goosen,[1] and Fred van Keulen[1]
[1]*Department of Precision and Microsystem Engineering, Delft University of Technology, Mekelweg 2, 2628CD Delft, The Netherlands*
[2]*Netherlands Organization for Applied Scientific Research, TNO, Delft, The Netherlands*

(Received 7 March 2017; accepted 13 June 2017; published online 29 June 2017)

Due to the harmonic motion of the cantilever in Tapping Mode Atomic Force Microscopy, it is seemingly impossible to estimate the tip-sample interactions from the motion of the cantilever. Not directly observing the interaction force, it is possible to damage the surface or the tip by applying an excessive mechanical load. The tip-sample interactions scale with the effective stiffness of the probe. Thus, the reduction of the mechanical load is usually limited by the manufacturability of low stiffness probes. However, the one-to-one relationship between spring constant and applied force only holds when higher modes of the cantilever are not excited. In this paper, it is shown that, by passively tuning higher modes of the cantilever, it is possible to reduce the peak repulsive force. These tuned probes can be dynamically more compliant than conventional probes with the same static spring constant. Both theoretical and experimental results show that a proper tuning of dynamic modes of cantilevers reduces the contact load and increases the sensitivity considerably. Moreover, due to the contribution of higher modes, the tuned cantilevers provide more information on the tip-sample interaction. This extra information from the higher harmonics can be used for mapping and possibly identification of material properties of samples. [http://dx.doi.org/10.1063/1.4990276]

I. INTRODUCTION

An Atomic Force Microscope (AFM) is a versatile instrument that enables measurement and manipulation of samples at the nanoscale. Recent advances in AFM technology already carried its application beyond topography imaging, such as subsurface elasticity measurements,[39] unfolding force measurements of biomolecules,[21] thermal conductivity measurements,[9,16] surface chemical composition mapping,[22] and mechanical properties mapping.[24] Nonetheless, topography imaging with Tapping Mode AFM (TM-AFM) can still be considered the most common application.

In TM-AFM, the cantilever is excited by a dithering signal with constant amplitude and a frequency near the fundamental resonance frequency of the cantilever. To prepare for scanning, the cantilever is brought in the vicinity of the sample surface until its amplitude decreases to a user-defined set-point amplitude. While scanning the surface, the amplitude is kept constant by adjusting the distance between the cantilever and the sample. The control signal that adjusts the distance is interpreted as the topography image. The phase delay between the motion of the cantilever and excitation signal is recorded as a measure of energy dissipation and can be related to adhesion, viscoelasticity, or hysteresis in the surface energy level.[5,34]

As shown in Fig. 1, in TM-AFM, the tip hits the sample surface in every cycle, experiencing both attractive and repulsive Tip-Sample Interaction (TSI) forces. Since these forces occur only during a fraction of a cycle, they affect the motion of the cantilever in a weakly nonlinear manner. Consequently, the motion of the cantilever remains harmonic.

Although some theoretical studies suggest that the motion of the cantilever should include effects of higher modes,[7,33] experiments show that effects of higher modes are negligible and most likely below the noise level.[2] Only in specific conditions, such as for extremely low Q factors (in the order of 1), the effects of higher modes could be experimentally detected. Even for low-Q measurements, the presence or detectability of the second harmonic is not guaranteed.[24] Thus, depending on the sample properties, noise level, operation parameters, etc., the higher harmonics may

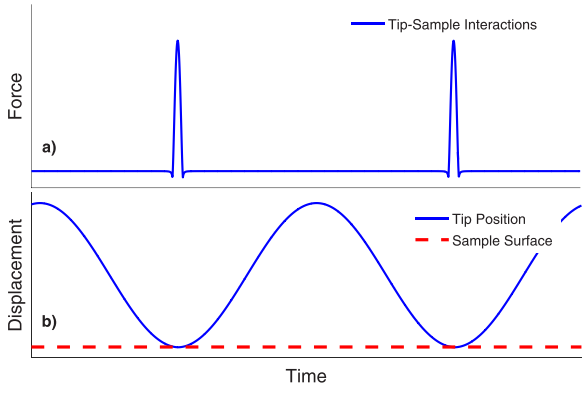

FIG. 1. (a) Tip-sample interactions, (b) dynamic motion of cantilever while touching the sample surface in TM-AFM (schematic).

[a)]Email: hamed.sadeghianmarnani@tno.nl

or may not be detected. Nonetheless, for the tapping mode AFM in air, the motion of the cantilever can be considered as purely harmonic as the higher harmonics are undetectable. Since a considerable amount of information on the TSI forces is modulated via the higher Fourier components, and the cantilever only vibrates with a single frequency, most of the information on the TSI force is lost in the noise.

The reason for a harmonic motion of the cantilever is well explained in the frequency domain.[25] Because of the large quality factor of the cantilever, its frequency response function (FRF) has orders of magnitude lower gain at frequencies other than the resonance frequency. Thus, similar to a sharp band pass filter, the cantilever only passes the frequency content of the TSI force, which corresponds to its resonance frequency and attenuates the higher frequency content. Consequently, the output, i.e., the cantilever's motion, can only have one dominant frequency component, and higher harmonics are likely to be obscured by the noise.

Since the motion of the cantilever remains harmonic, the TSI force affects the cantilever as a weak nonlinearity and the amplitude and phase of the cantilever motion only evolve with the periodic average of the TSI force.[12,13,29,37] Therefore, only the information on the periodic average of the tip-sample interaction can be extracted. On the other hand, damage does not occur due to the average of the TSI force but due to the maximum repulsive force, referred to as Peak Repulsive Force (PRF).[36] Since it is not possible to directly measure the PRF or extract it from the periodic average of the TSI force, it is not possible to directly control it. Consequently, there is always a probability of damage in TM-AFM. In industrial applications of AFM such as metrology,[11,26,27] it is important to avoid any damage to the sample.

To reduce the damage probability, it is wise to use the most compliant cantilever available and choose proper operation parameters, i.e., amplitude and frequency set points.[36] However, the reduction of the TSI force via these methods is limited because of other practical issues, such as fabrication limits or high noise in compliant cantilevers. To capture more information on the TSI force, the motion of a cantilever should contain multiple frequency components. For this reason, either the input (dither signal) or the system (cantilever and environment) has to be altered. Both options have already been explored. The first method is to introduce an auxiliary excitation signal with a different frequency, which is called the "multi-modal" operation mode.[8] The second method is based on adjusting the system using multi-harmonic cantilevers[30] or operating in a fluid environment.[24] Next, some researchers utilized the sub-harmonic (static) motion to map binding sites of biological samples, known as Topography and RECognition (TREC) mode.[23] It must be mentioned that the TREC mode is not a general imaging technique, but rather a particular method to detect chemical binding sites of biological samples, and without the presence of the binding forces, the sub-harmonic motion of the cantilever is negligible or below the noise level.

As mentioned, the Multi-modal AFM[8,20] introduces an auxiliary excitation signal to excite one or more higher modes of the cantilever simultaneously. Multiple lock-in amplifiers are utilized to measure the amplitude and phase of the different modes (typically first and second bending modes). Consequently, two images per mode are available, i.e., amplitude and phase. The images gathered with the multimode AFM technique demonstrate that some information is modulated on higher modes, which could not be extracted with standard tapping mode AFM.[8] However, the external excitation of higher modes introduces both super and sub-harmonic frequency contents. The extra energy in the second mode reciprocally increases and decreases the nanoindentation in different cycles. Thus, even a subtle amplitude of the second mode can cause a fluctuating TSI force on the sample surface, which might be damaging.

The second option to acquire more information is to change the system. This can be done either by decreasing the Q factor[2] (via operating in liquid) or by increasing the response of the higher modes of the cantilever by introducing additional resonating parts to the cantilever, so-called harmonic cantilevers or force sensing cantilevers.[30–32] Since the TSI force contains peaks at integer multiples of the excitation frequency,[33] the secondary resonator can capture some of the higher frequency content of the TSI force. For example, Sahin *et al.* introduced a cantilever that has a cutout in its neck to tailor the ratio between the first and the third modes.[31] They demonstrated that when the resonance frequency of the third mode is exactly 16 times the first resonance frequency, more information on the sample elasticity is modulated in the third mode. Sahin *et al.* utilized the first torsional mode of the cantilever to measure the interaction force.[30] Sarioglu *et al.* patterned comb-like trenches on the cantilever to realize the second resonator and acquire more information using an interferometer.[32] For the same purpose, Li *et al.* suggested to attach a lumped mass particle to the cantilever[17] to adjust its dynamic properties. Felts and King introduced gaps inside the cantilever and showed that the ratio between the first and second resonance could be changed considerably.[6] Xia *et al.* utilized a level set optimization method to optimize the cantilever for bi-harmonic methods.[38] Lately, Loganathan and Bristow designed a bi-harmonic probe for which the second resonance frequency is two times the fundamental one. Their design consists of two cantilevers, one inside the other, and presents considerably higher force sensitivity in comparison to normal cantilevers.[19]

The approaches as mentioned above indeed gather more information on the sample. However, these designs are geometrically complex, which limits their feasibility regarding fabrication of smaller cantilevers. It is well known that in order to decrease the tip-sample forces, increase the force sensitivity, and increase the imaging speed, it is necessary to scale down the dimensions of cantilevers as much as possible,[18] which requires a simple design. Moreover, it is not entirely understood how the multi-harmonic cantilevers affect the TSI force. For example, some of them might increase and others might reduce the PRF.

In this paper, we aim to reduce the TSI force with an easily scalable minimalistic change in the geometry of the cantilever. For this purpose, we propose to tune the second vibration mode of the cantilever with respect to its first

mode. As a result, the second mode of the cantilever gets excited by one of the super-harmonic components of the TSI force and provides more information on the mechanical properties of the sample. Also, by choosing an even number (6) as the frequency ratio, the first and the second modes of the cantilever get self-synchronized, which considerably reduces the PRF and, consequently, the probability of damaging the surface or the tip.

This paper is organized as follows: Sec. II presents the design of dynamically tuned cantilevers, Sec. III describes the TSI force and the working principle of the proposed probe, and Sec. IV demonstrates the performance of the cantilever via experimental results. The conclusions are presented in Sec. V.

II. TUNING THE DYNAMICS OF CANTILEVERS

As mentioned in the Introduction section, the TSI force in the time domain contains periodic impulse-like functions. In the frequency domain, such a periodic impulse-like function includes a large number of super-harmonic components with integer multiples of the excitation frequency. As long as none of these components coincide with any resonance frequencies of the cantilever, their effect is usually undetectable and the motion of the cantilever is nearly harmonic. In this section, we propose to change the geometry of the cantilever such that its second bending mode coincides with the 6th super-harmonic component of the force. Consequently, the second bending mode will also be excited by the TSI force.

For prismatic cantilevers—provided that the Euler-Bernoulli beam theory holds—the resonance frequency of the second bending mode is approximately 6.267 times the first resonance frequency. Considering that the ratio between the first and second resonance frequencies of a prismatic cantilever is close to 6, a relatively small adjustment in shape can change this ratio to exactly 6. To tune the cantilever, we propose a trapezoidal geometry for which the width is a linear function of the axial coordinate.

Considering a homogeneous isotropic material, and the Euler-Bernoulli beam theory, the free vibration of the cantilever can be described with the following non-dimensional eigenvalue problem:

$$\left[\frac{\partial^2}{\partial x^2}\left(b(x)\frac{\partial^2}{\partial x^2}\right) - b(x)\lambda_i^2\right]\phi_i(x) = 0, \qquad (1)$$

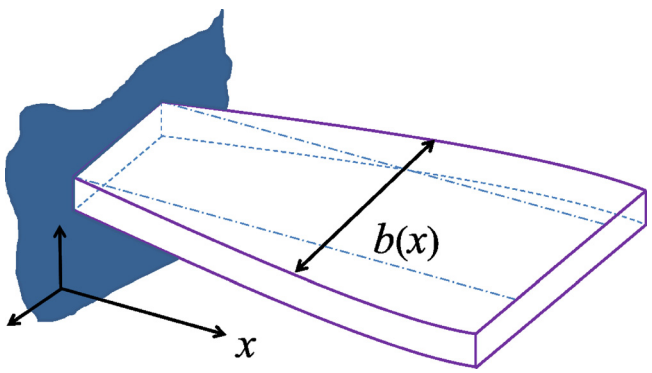

FIG. 2. Schematic view of the cantilever with variable width.

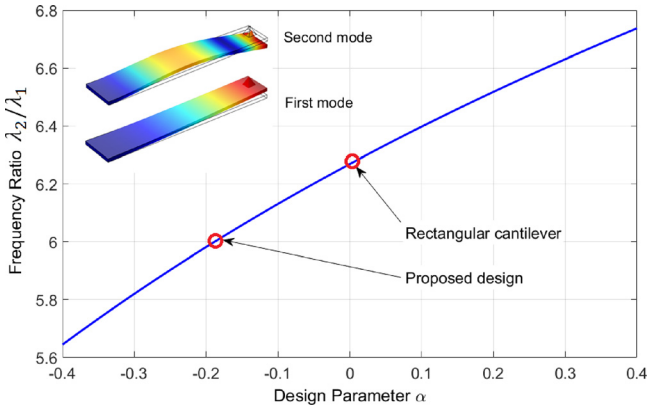

FIG. 3. Frequency ratio of first two modes of the cantilever versus the design parameter α (i.e., the ratio of obliqueness of the cantilever).

where x, λ_i, and $\phi_i(x)$ represent the non-dimensional axial coordinate, ith eigen frequency, and ith bending mode, respectively. The width of the cantilever ($b(x)$, see Fig. 2) is normalized with respect to the width at the clamping. A linear variation of the width $b(x) = 1 + \alpha x$ is chosen, in which α is a design parameter. The eigenvalue problem Eq. (1) has been solved using the well-known Galerkin method. Figure 3 shows the frequency ratio as a function of the design parameter α, along with the corresponding mode shapes. As can be seen in Fig. 3, if $\alpha = -0.18$, i.e., the cantilever is slightly trapezoidal, the frequency of the second mode is 6 times the frequency of the first mode. It must be mentioned that in Eq. (1), the torsional modes, in-plane modes, bending modes in lateral direction, and effects of tip mass are completely ignored. Although the torsional modes are not excited and in-plane modes have much higher frequency, a 3D finite element method was used to validate the method and correct for the tip mass by fine-tuning the design parameter.

III. TIP-SAMPLE INTERACTIONS FOR TUNED CANTILEVERS

In this section, we shall discuss the dynamic behavior of the tuned cantilever in comparison with a standard cantilever. Figures 4(a) and 4(c) show the TSI force and tip motion in the frequency domain, calculated from a full nonlinear simulation. The point frequency response functions (FRF) for the cantilever's tip (Red) are also included to demonstrate the effects of dynamic tuning. Figures 4(b) and 4(d) show the SEM images of the corresponding cantilevers.

Since the frequency of the forced vibration only depends on the excitation frequency (and not on the eigenfrequencies of the cantilever), irrespective of the tuning, the motion of the cantilever can contain only the frequencies that are exact integer multiples of the excitation frequency (so-called harmonic and super-harmonic components). In theory, any cantilever is vibrating with all the integer multiples of the excitation frequency. But, if the vibration modes are not tuned, the amplitude of super-harmonic components is negligibly small. The proposed tuning shifts the second bending mode of the cantilever (second peak of FRF) to the frequency of the 6th Fourier component of the TSI force,

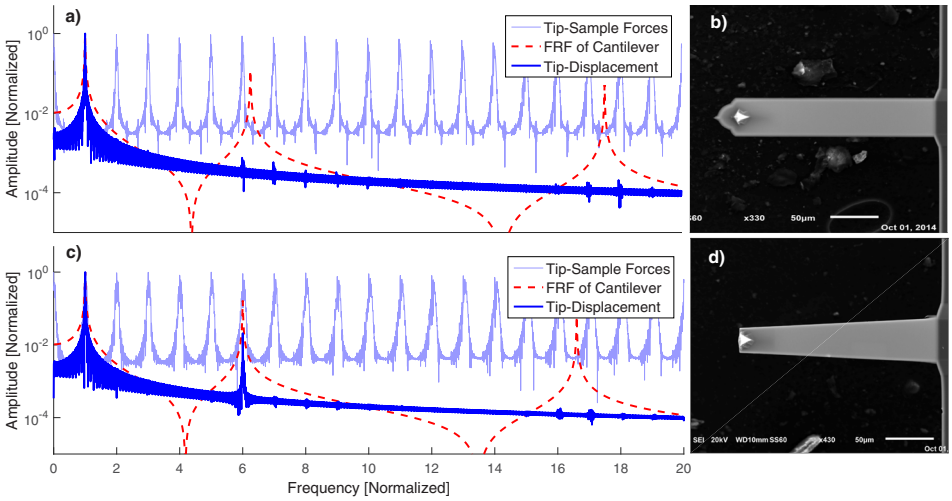

FIG. 4. (a) Simulated tip-sample interaction, FRF of the cantilever, and motion of the tip in the frequency domain for rectangular cantilever; (b) SEM image of the commercially available MPP-22120 cantilever used in simulations and experiments; (c) simulated tip-sample interaction, FRF of the cantilever, and motion of the tip in the frequency domain for the tuned cantilever; (d) SEM image of the custom made tuned cantilever.

thereby increasing the amplitude of the 6th super-harmonic motion.

To demonstrate only the effect of shape, Fig. 5 compares the simulated TSI force for rectangular and trapezoidal cantilevers, while both cantilevers have the same spring constant (5 N m^{-1}), same first resonance frequency (100 kHz), and same quality factor (100). The motion of the proposed cantilever is not harmonic, but a superposition of two harmonic components, as shown in Fig. 5. The phase of the motion of the first and the second modes is synchronized in a way that the speed of the tip is reduced right before touching the sample surface. Hence, the proposed cantilever indents the sample less and, consequently, applies a lower TSI force.

The reduction in the approach velocity and the TSI force is caused by self-synchronization of the two modes of the cantilevers. The frequency ratio of the cantilever motion is an exact integer number; therefore, the motion of the cantilever remains periodic. In other words, since the second mode is purely excited with the TSI force, its phase with respect to the first mode in steady state conditions does not change from one cycle to the other. This phase synchronization happens such that the contribution of the second mode reduces the indentation.

Notice that the effects of long-range nonlinear forces such as electrostatic attraction and squeeze film effects can influence the resonance frequencies and degrade the performance of the cantilever. However, these effects are negligible in comparison to the TSI force. Thus, to avoid unnecessary complications, it is reasonable to ignore them while tuning the cantilever for TM-AFM in air or vacuum.

To quantify the force reduction for tuned cantilevers, we calculate the peak repulsive forces using a multi-harmonic extension of the periodic averaging method. Since the mathematical details of the periodic averaging method are not in the scope of this paper, we only present the final results. More information on the periodic averaging method for AFM cantilevers is available in Ref. 12. Figure 6 shows the peak repulsive forces versus the amplitude set-point for a test case with dynamic characteristics as indicated in the caption. As can be seen, the peak repulsive force for the tuned cantilever is on average 70% less than for a conventional cantilever.

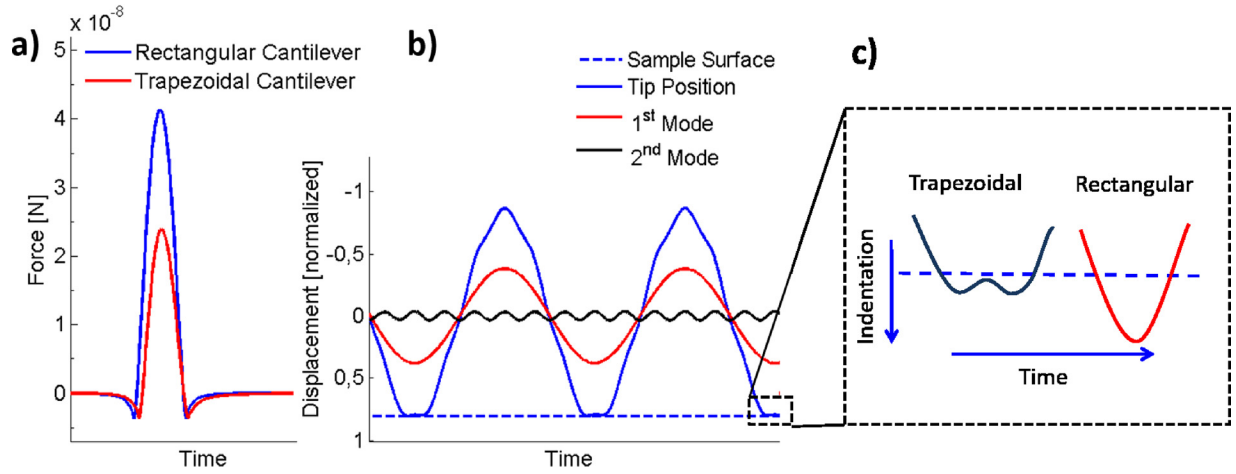

FIG. 5. (a) Tip-sample interactions in single period for rectangular and trapezoidal cantilevers. (b) Tip-motion and mode participation of first and second modes for tuned cantilevers. (c) Schematic explanation for reduction of indentation with tuned cantilevers. The second mode of the cantilever retracts the tip during the indentation. In the simulation, the free air amplitude was 50 nm, and the amplitude set-point was 40 nm (amplitude ratio 80%).

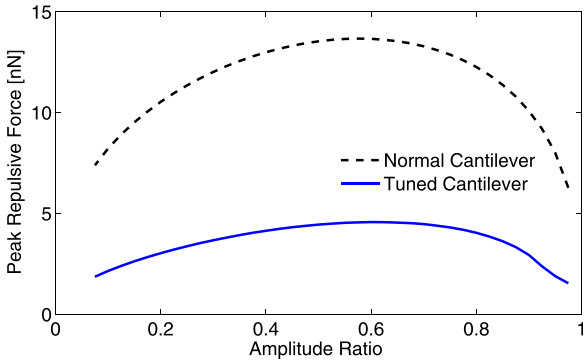

FIG. 6. Calculated peak repulsive force versus amplitude ratio for a free air amplitude of 50 nm and tip radius 10 nm, spring constant 1 N/m and quality factor Q1 = 100 and Q2 = 150, considering the Derjaguin-Muller-Toporov[4] modulus of silicon tip and silicon sample.

IV. EXPERIMENTAL RESULTS AND DISCUSSION

To fabricate and test a tuned cantilever as a proof of concept, a commercially available probe [Veeco MPP-22120, Fig. 4(b)] was patterned with a Gallium Focused Ion Beam (Ga-FIB) to the desired shape [Fig. 4(d)]. The dynamic properties of the cantilever were measured before and after the patterning using the thermal calibration method[3] and are presented in Table I. Here we shall first present the imaging performance of the proposed cantilever and verify the feasibility of extracting information from higher harmonics. Second, we demonstrate the reduction in the TSI force via a force measurement experiment and an apparent height test.

A. Imaging performance

To evaluate the imaging performance of the proposed cantilever, Fig. 7 shows the AFM images of a commercially available two-phase polymer sample (PS-LDPE, Bruker). The images are captured with the two cantilevers under the same imaging conditions and set-points using a Bruker Dimension Fastscan AFM. For both cantilevers, the peak amplitude was set to ≈240 nm, the excitation frequency and the free air amplitude were chosen to be 7% below the resonance, the set point amplitude was ≈150 nm, and the scanning speed for both cases was 38.8 μm/s. For a fair comparison, the image processing is limited to a first order offset elimination in the height images, and zero-shifting the color bar relative to the minimum of the data (i.e., the color bars all start at zero). As shown in Fig. 7, the phase image with the tuned cantilever has considerably higher contrast, while there is hardly any difference between the amplitude images. Since the stiffness of the two probes is in the same order, the extreme increase in phase sensitivity can only be explained by the dynamically increased force sensitivity. The ratio between viscoelasticity and elasticity of the sample surface affects the phase of the TSI. Since the tuned cantilever is dynamically more sensitive to the TSI force, it responds more aggressively to changes in the phase of the force as well. Consequently, the phase image captured with the dynamically tuned cantilever has more contrast in comparison to the one obtained with the standard cantilever.

TABLE I. Dynamic properties of the cantilever before and after patterning.

	k (N/m)	ω_1 (kHz)	ω_2(kHz)	Q_1	Q_2	$\frac{\omega_2}{\omega_1}$
Before patterning	1.19	40.86	281.77	136	278	6.89
After patterning	0.87	50.50	307.28	142	274	6.08

As mentioned in Sec. III, the second mode is purely excited by the TSI force. Since different frequency components contain different information on the TSI force, the motion of the second mode provides additional information on the sample, which is not available from the first mode. This additional information can be extracted using an auxiliary lock-in amplifier. Figure 8 shows the images gathered from the second bending mode of the cantilever. Clearly, for the tuned cantilever, the amplitude and phase of the second mode also provide information on the mechanical properties of the sample. Yet, a general mathematical calculation is needed to estimate the material properties from amplitude and phase signals. In this context, Raman *et al*. have shown that an approximate stiffness measurement is possible using the harmonic balancing method.[24] The extra information provided by the second mode of the cantilever can also be useful in determining a more accurate height of sub-manometer structures.[15] In our experiments, we only excite the first mode of the cantilever to allow for the self-synchronization to reduce the force. However, it is also possible to use the proposed cantilever in a bi-modal AFM configuration, while preserving the periodicity of the motion. It is known that the periodicity simplifies the theoretical analysis and improves the accuracy of quantitative measurements.[14]

B. Force measurement

To verify the reduction of the forces with tuned cantilevers, we perform the experiment as suggested by Tamer *et al*.[28,35] in which a force sensor is placed under the cantilever instead of the sample surface, as shown in Fig. 9. The force sensor itself is also a micro-cantilever with its own optical readout system. The force sensing cantilever has a much higher resonance frequency in comparison to the imaging cantilever (1.29 MHz and 50 kHz, respectively). Hence, the first few frequency components of the TSI force fall into the static regime of the sensing cantilever and can be measured. We aim to compare those frequency components in the motion of the sensing cantilever, if the two different cantilevers tap on the sensor. To make a correct comparison, we ensured that the sensitivity of the force sensor is the same in both experiments by, first, tapping exactly on the same specific spot on the sensing cantilever (the sensing spot in Fig. 9), and second, measuring the thermal noise of the force sensor before and after every experiment and check for any possible drift in the optical sensitivity.

For all of the experiments in this section, we chose a peak amplitude of 80 nm. The excitation frequency is chosen such that the free air amplitude is 4% less than the peak amplitude (76.8 nm). Figure 10 shows the deflection of the

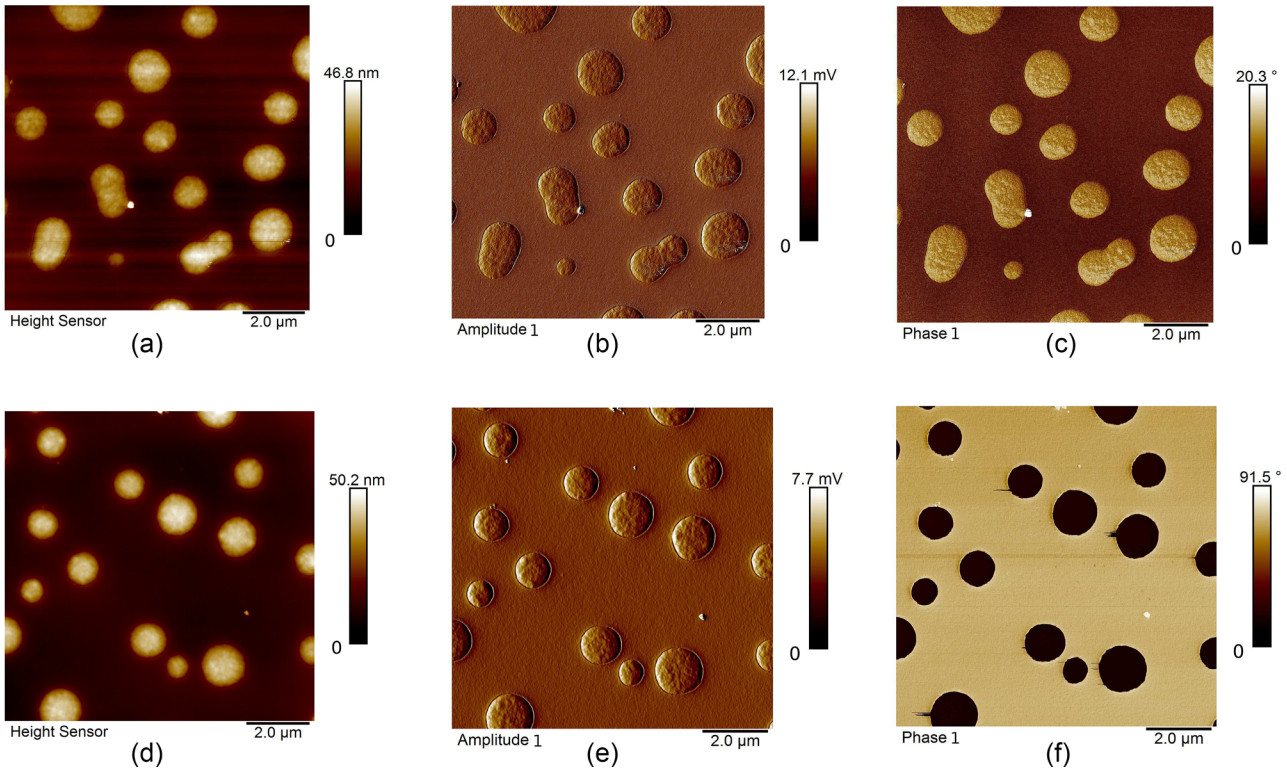

FIG. 7. Topography (measured via height sensors), amplitude error, and phase images of a PS-LDPE sample gathered with the MPP22120 cantilever and the tuned cantilever.

imaging cantilever (in this case the tuned cantilever), in frequency and time domain, while the imaging cantilever is tapping on the sensing spot (with amplitude ratio of 60%). The inherent noise of the force sensing cantilever is measured, while the two cantilevers are disengaged.

As can be seen, the deflection of the tuned cantilever contains the first and sixth harmonic of the excitation frequency, together with some other small peaks at the integer multiples of the excitation frequency. The signal from the force sensing cantilever contains first few (23 in this case) of

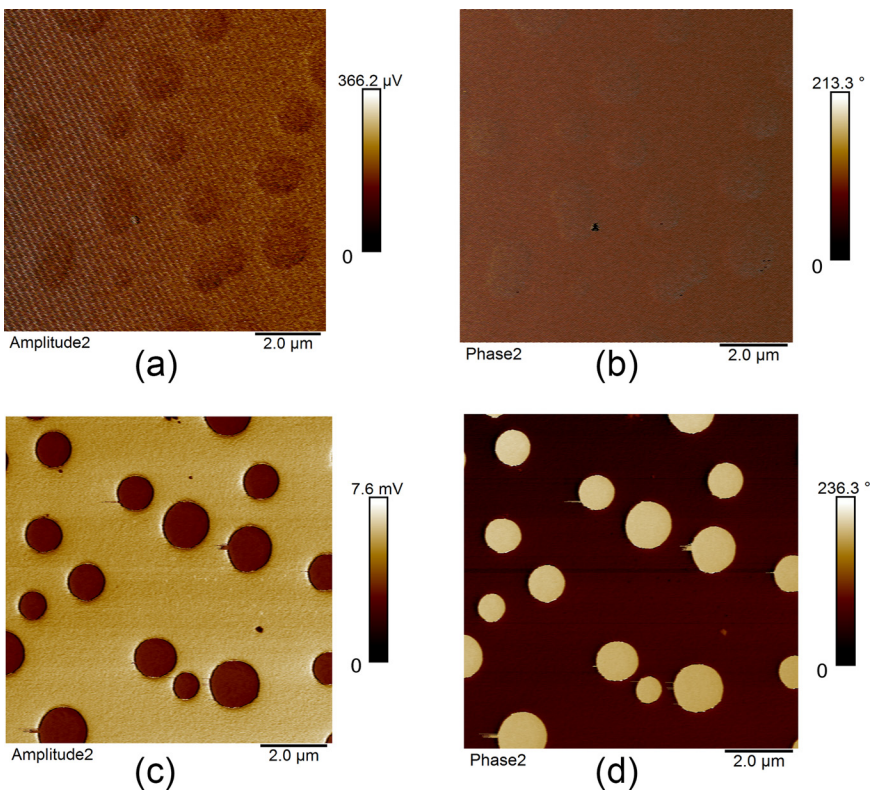

FIG. 8. AFM images of PS-LDPE sample gathered with the MPP22120 cantilever and the tuned cantilever captured from the second mode of vibration using an auxiliary lock-in amplifier.

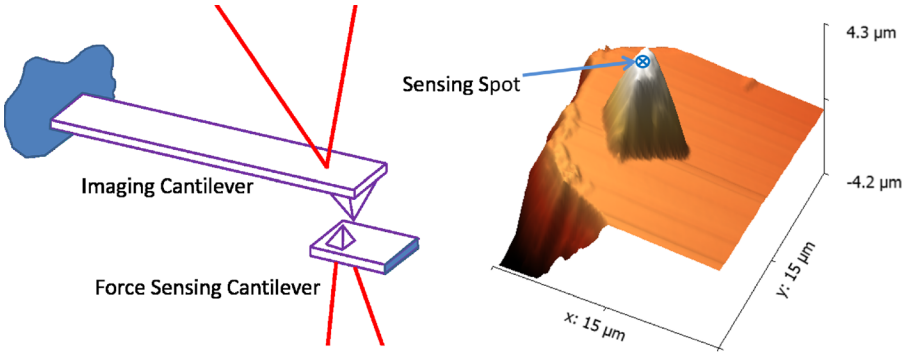

FIG. 9. Schematic of the force sensing technique and the image of the tip of the sensing cantilever, which is captured with the imaging cantilever.

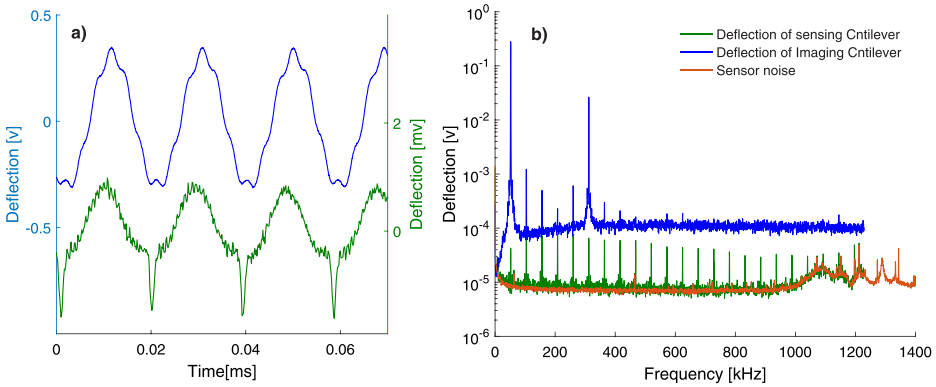

FIG. 10. Measured signal of the optical sensor from the imaging and the sensing cantilevers, (a) in time domain and (b) in frequency domain.

the super-harmonic contents of the TSI force. Since the deflection of the force sensing cantilever exhibits its own noise and there exists a large amount of phase distortion between different frequency contents of the motion, the TSI force itself cannot be resolved in the time domain. Therefore, to compare the forces applied with a tuned and a conventional cantilever, we only measure the peaks in the frequency domain of the sensing cantilever and calculate their L_2 norm. The L_2 norm of a signal is the same in both time and frequency domains and represents a measure of power transmitted with the signal. Figure 11 shows the results of this experiment with the two cantilevers mentioned in Table I at different amplitude set points. As can be seen, the power transmitted to the force sensing cantilever is much lower when a tuned cantilever is used. Although no calibrated TSI forces could be measured in real-time, the results in Fig. 11 consistently with the results in Fig. 6 confirm the reduction of the TSI forces with tuned cantilevers.

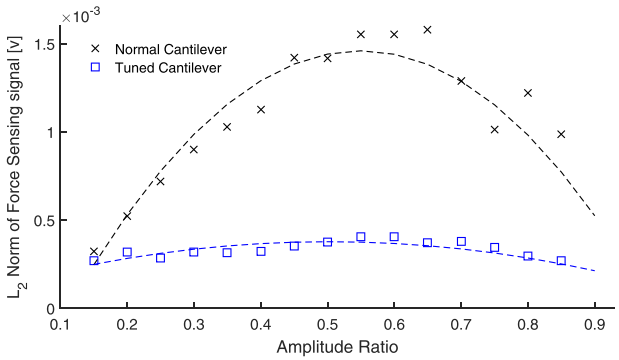

FIG. 11. L_2 norm of the force sensor signal, as a measure of the TSI force, measured from the cantilevers in Table I. Dashed lines show a quadratic data fit.

C. Apparent height image of DNA

As mentioned previously, the forces in TM-AFM are not directly accessible from experiments. However, the apparent height of soft nanoscale samples can give an estimate of the average repulsive forces. In tapping mode AFM, the repulsive forces compress the samples. Consequently, the apparent height of samples is commonly lower than their real values. Antognozzi *et al.*[1] presented a height histogram of a double-stranded DNA, which was captured with TM-AFM and compared it with shear-mode AFM. Since the shear-mode AFM reduces the repulsive forces, a higher average height was observed in comparison to TM-AFM (1 nm for shear AFM and 0.6 nm for TM-AFM[40]). We use the same method to compare the average of TSI force for dynamically tuned and standard cantilevers. Figure 12(a) shows the height image of a double-stranded DNA imaged in TM-AFM using a tuned probe in air. Figure 12(a) compares the height histogram measured with the tuned cantilever with those measured by Antognozzi *et al.*[1] in shear mode AFM and TM AFM. As shown in Fig. 12, using the tuned cantilevers in TM-AFM, even a higher average height could be observed (1.2 nm), which is closer to its actual value [theoretical value 2.2 nm and X-ray measurement 2.0 nm (Ref. 10)]. Consistently, the increased average apparent height suggests that the tuning of the second mode reduces the repulsive forces.

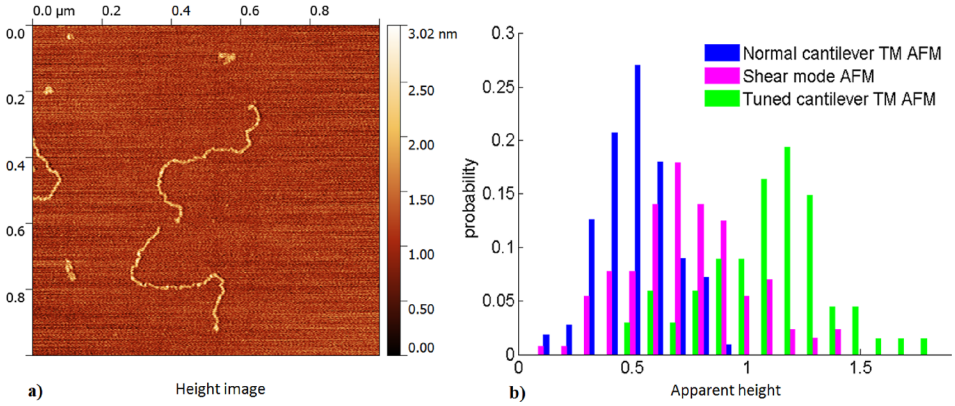

FIG. 12. (a) Height image of DNA on a mica surface captured with a tuned cantilever in tapping mode in air. Free air amplitude and working amplitude were ≈30 nm and ≈25 nm, respectively, (b) Height histogram of the DNA on a mica sample, a comparison of TM AFM with normal cantilevers, and shear mode AFM and TM AFM with tuned cantilever.

V. CONCLUSION

In this paper, a minor adjustment of the AFM cantilever geometry has been suggested to tune its vibration modes. Such a cantilever utilizes its second mode to enhance imaging performance by capturing the 6th super-harmonic force component. Theoretical and experimental results demonstrate that it benefits from reduced tip-sample interaction forces and increased sensitivity in tapping mode AFM. At the same time, the proposed cantilever provides additional information modulated via the second bending mode, which can be used to extract mechanical properties of the samples. The tapered cantilever is an easily scaled design, which enables more sensitive imaging with higher contrast in material properties mapping while applying lower TSI forces, thus reducing the tip damage or the sample distortion.

ACKNOWLEDGMENTS

This work was supported by Netherlands Organization for Applied Scientific Research, TNO, Early Research Program 3D Nanomanufacturing. The authors acknowledge Ir. Hozanna Miro from Kavli Nanolab Delft, for her help in fabricating the cantilever.

[1]M. Antognozzi, M. D. Szczelkun, A. N. Round, and M. J. Miles, "Comparison between shear force and tapping mode AFM-high resolution imaging of DNA," Single Mol. **3**(2–3), 105–110 (2002).
[2]S. Basak and A. Raman, "Dynamics of tapping mode atomic force microscopy in liquids: Theory and experiments," Appl. Phys. Lett. **91**(6), 064107 (2007).
[3]N. Burnham, X. Chen, C. Hodges, G. Matei, E. Thoreson, C. Roberts, M. Davies, and S. Tendler, "Comparison of calibration methods for atomic-force microscopy cantilevers," Nanotechnology **14**(1), 1 (2003).
[4]H.-J. Butt, B. Cappella, and M. Kappl, "Force measurements with the atomic force microscope: Technique, interpretation and applications," Surf. Sci. Rep. **59**(1), 1–152 (2005).
[5]J. Cleveland, B. Anczykowski, A. Schmid, and V. Elings, "Energy dissipation in tapping-mode atomic force microscopy," Appl. Phys. Lett. **72**(20), 2613–2615 (1998).
[6]J. R. Felts and W. P. King, "Mechanical design for tailoring the resonance harmonics of an atomic force microscope cantilever during tip–surface contact," J. Micromech. Microeng. **19**(11), 115008 (2009).
[7]K. Gadelrab, S. Santos, J. Font, and M. Chiesa, "Single cycle and transient force measurements in dynamic atomic force microscopy," Nanoscale **5**(22), 10776–10793 (2013).
[8]R. Garcia and E. T. Herruzo, "The emergence of multifrequency force microscopy," Nat. Nanotechnol. **7**(4), 217–226 (2012).
[9]R. Grover, B. McCarthy, D. Sarid, and I. Guven, "Mapping thermal conductivity using bimetallic atomic force microscopy probes," Appl. Phys. Lett. **88**(23), 233501 (2006).
[10]H. G. Hansma, D. Laney, M. Bezanilla, R. L. Sinsheimer, and P. K. Hansma, "Applications for atomic force microscopy of DNA," Biophys. J. **68**(5), 1672–1677 (1995).
[11]R. Herfst, B. Dekker, G. Witvoet, W. Crowcombe, D. de Lange, and H. Sadeghian, "A miniaturized, high frequency mechanical scanner for high speed atomic force microscope using suspension on dynamically determined points," Rev. Sci. Instrum. **86**(11), 113703 (2015).
[12]S. Hu and A. Raman, "Analytical formulas and scaling laws for peak interaction forces in dynamic atomic force microscopy," Appl. Phys. Lett. **91**(12), 123106 (2007).
[13]S. Hu and A. Raman, "Inverting amplitude and phase to reconstruct tip–-sample interaction forces in tapping mode atomic force microscopy," Nanotechnology **19**(37), 375704 (2008).
[14]C.-Y. Lai, V. Barcons, S. Santos, and M. Chiesa, "Periodicity in bimodal atomic force microscopy," J. Appl. Phys. **118**(4), 044905 (2015).
[15]C.-Y. Lai, S. Santos, and M. Chiesa, "Reconstruction of height of sub-nanometer steps with bimodal atomic force microscopy," Nanotechnology **27**(7), 075701 (2016).
[16]J.-H. Lee and Y. Gianchandani, "High-resolution scanning thermal probe with servocontrolled interface circuit for microcalorimetry and other applications," Rev. Sci. Instrum. **75**(5), 1222–1227 (2004).
[17]H. Li, Y. Chen, and L. Dai, "Concentrated-mass cantilever enhances multiple harmonics in tapping-mode atomic force microscopy," Appl. Phys. Lett. **92**(15), 151903 (2008).
[18]M. Li, H. X. Tang, and M. L. Roukes, "Ultra-sensitive NEMS-based cantilevers for sensing, scanned probe and very high-frequency applications," Nat. Nanotechnol. **2**(2), 114–120 (2007).
[19]M. Loganathan and D. A. Bristow, "Bi-harmonic cantilever design for improved measurement sensitivity in tapping-mode atomic force microscopy," Rev. Sci. Instrum. **85**(4), 043703 (2014).
[20]J. R. Lozano and R. Garcia, "Theory of multifrequency atomic force microscopy," Phys. Rev. Lett. **100**(7), 076102 (2008).
[21]K. C. Neuman and A. Nagy, "Single-molecule force spectroscopy: Optical tweezers, magnetic tweezers and atomic force microscopy," Nat. Methods **5**(6), 491 (2008).
[22]A. Noy, D. V. Vezenov, and C. M. Lieber, "Chemical force microscopy," Annu. Rev. Mater. Sci. **27**(1), 381–421 (1997).
[23]J. Preiner, A. Ebner, L. Chtcheglova, R. Zhu, and P. Hinterdorfer, "Simultaneous topography and recognition imaging: Physical aspects and optimal imaging conditions," Nanotechnology **20**(21), 215103 (2009).
[24]A. Raman, S. Trigueros, A. Cartagena, A. Stevenson, M. Susilo, E. Nauman, and S. A. Contera, "Mapping nanomechanical properties of live cells using multi-harmonic atomic force microscopy," Nat. Nanotechnol. **6**(12), 809–814 (2011).
[25]T. R. Rodriguez and R. Garcia, "Tip motion in amplitude modulation (tapping-mode) atomic-force microscopy: Comparison between continuous and point-mass models," Appl. Phys. Lett. **80**(9), 1646–1648 (2002).
[26]H. Sadeghian, R. Herfst, B. Dekker, J. Winters, T. Bijnagte, and R. Rijnbeek, "High-throughput atomic force microscopes operating in parallel," Rev. Sci. Instrum. **88**(3), 033703 (2017).
[27]H. Sadeghian, R. Herfst, J. Winters, W. Crowcombe, G. Kramer, T. van den Dool, and M. H. van Es, "Development of a detachable high speed miniature scanning probe microscope for large area substrates inspection," Rev. Sci. Instrum. **86**(11), 113706 (2015).
[28]H. Sadeghian and M. S. Tamer, European patent 15181449.8 (2017).

[29]J. E. Sader, T. Uchihashi, M. J. Higgins, A. Farrell, Y. Nakayama, and S. P. Jarvis, "Quantitative force measurements using frequency modulation atomic force microscopy theoretical foundations," Nanotechnology **16**(3), S94 (2005).
[30]O. Sahin, S. Magonov, C. Su, C. F. Quate, and O. Solgaard, "An atomic force microscope tip designed to measure time-varying nanomechanical forces," Nat. Nanotechnol. **2**(8), 507–514 (2007).
[31]O. Sahin, G. Yaralioglu, R. Grow, S. Zappe, A. Atalar, C. Quate, and O. Solgaard, "High-resolution imaging of elastic properties using harmonic cantilevers," Sens. Actuators, A **114**(2), 183–190 (2004).
[32]A. F. Sarioglu, M. Liu, and O. Solgaard, "High-resolution nanomechanical mapping using interferometric-force-sensing AFM probes," J. Microelectromech. Syst. **20**(3), 654–664 (2011).
[33]R. W. Stark, G. Schitter, M. Stark, R. Guckenberger, and A. Stemmer, "State-space model of freely vibrating and surface-coupled cantilever dynamics in atomic force microscopy," Phys. Rev. B **69**(8), 085412 (2004).
[34]J. Tamayo and R. Garcia, "Relationship between phase shift and energy dissipation in tapping-mode scanning force microscopy," Appl. Phys. Lett. **73**(20), 2926–2928 (1998).
[35]M. S. Tamer, H. Sadeghian, A. Keyvani, H. Goosen, and F. van Keulen, "Quantitative measurement of tip-sample interaction forces in tapping mode atomic force microscopy," in *Proceedings of the 13th International Workshop on Nanomechanical Sensing* (2016), pp. 199–200.
[36]V. Vahdat and R. W. Carpick, "Practical method to limit tip–sample contact stress and prevent wear in amplitude modulation atomic force microscopy," ACS Nano **7**(11), 9836–9850 (2013).
[37]L. Wang, "Analytical descriptions of the tapping-mode atomic force microscopy response," Appl. Phys. Lett. **73**(25), 3781–3783 (1998).
[38]Q. Xia, T. Zhou, M. Y. Wang, and T. Shi, "Shape and topology optimization for tailoring the ratio between two flexural eigenfrequencies of atomic force microscopy cantilever probe," Front. Mech. Eng. **9**(1), 50–57 (2014).
[39]K. Yamanaka, H. Ogiso, and O. Kolosov, "Ultrasonic force microscopy for nanometer resolution subsurface imaging," Appl. Phys. Lett. **64**(2), 178–180 (1994).
[40]C.-W. Yang, S. Hwang, Y. F. Chen, C. S. Chang, and D. P. Tsai, "Imaging of soft matter with tapping-mode atomic force microscopy and non-contact-mode atomic force microscopy," Nanotechnology **18**(8), 084009 (2007).